Toward the modelling of laminated veneer lumber stiffness and the influence of the number of plies

A. Peignon[1] · J. Serra[1] · A. Cantarel[1] · F. Eyma[1] · B. Castanié[1]

Abstract

This research paper studies the influence that the number of plies has on the identification of the mechanical properties of poplar Laminated Veneer Lumber (LVL) from tensile tests such as its stiffness. LVL poplar specimens were prepared with different ply configurations and subjected to uniaxial tensile tests. Both longitudinal and transverse stiffnesses were characterized in this research. The results show that the ply configuration influences the mechanical properties. The influence of the glued faces, the presence of lathe checks, and the compression ratio of veneers were studied during the manufacturing of the LVL. All these results provide valuable information for the design and optimization of laminated wood structures. An analytical modelling strategy is proposed to account for the effect of ply numbers, ply orientations, the compression ratio of veneers and the glue used on the stiffness of poplar laminate both in longitudinal and transverse directions.

Introduction

The use of wood in the transport industry is not new (Castanié et al. 2020, 2024) and it could become a solution to current environmental problems. Thanks to its low cost, low carbon footprint, and light weight, wood seems to be a good alternative to many materials (Mair-Bauernfeind et al. 2020). Laminated Veneer Lumber (LVL) and plywood are structural composite materials crafted from thinly peeled wood sheets, known as veneers, bonded using adhesive. While both share this fundamental construction, plywood distinguishes itself through a consistent cross-lamination pattern. This involves alternating longitudinal and transverse veneers throughout the laminate (Finnish Woodworking Industries Federation 2019). The manufacturing process of LVL and plywood permits careful selection of veneers devoid of defects. Remarkably, their static mechanical properties are on a par with or surpass those

✉ B. Castanié
bruno.castanie@insa-toulouse.fr

1 CNRS UMR 5312, INSA, ISAE-Supaéro, UPS, IMT Mines Albi, Institut Clément Ader (ICA), University of Toulouse, Toulouse, France

of solid wood (Leicester and Bunker 1969; Youngquist et al. 1984; Sasaki and Abdullahi 2001; Kiliç et al. 2010). Furthermore, recent research indicates that LVL exhibits noteworthy mechanical potential for applications involving crash and impact scenarios (Susainathan et al. 2019; Guélou et al. 2021a, b, 2022a, b).

However, plywood, LVL, and more generally wood plies are heterogeneous which leads to variation and a certain variability in mechanical properties (Guélou et al. 2021b). It is therefore essential to analyse them in detail to consider their use as a structural material in transport, e.g. in the automotive industry (WOOD Car 2021) or aeronautics (AURA AERO 2023).

Regarding the characterization of LVL, many studied the effect of the number of plies on a constant thickness LVL made with veneers of different thicknesses. For example, Kiliç et al. (2006) compare two LVLs of glutinous alder which are 20 mm thick, made from 2 to 4 mm-thick veneers using two different glues. They show that under shear, compression and bending, the breaking strength is greater for LVL made with 2 mm plies than for those made with 4 mm plies, regardless of the glue used. They also show that the longitudinal Young's modulus is higher in this configuration. They attribute this to the increasing amount of glue in LVL made from finer plies.

According to the literature, the number of plies in an LVL influences its stiffness or flexural strength. The explanations put forward are as follows: a better distribution of wood defects through veneers and a greater amount of glue in the LVL with the increase in the number of plies (Schaffer et al. 1972; Hoover et al. 1987; H'ng et al. 2010; Daoui et al. 2011).

On tensile tests, other authors show a similar relationship between the mechanical properties and the number of plies of the laminated veneer lumber. Youngquist et al. (1984) show an increase in stiffness and specific average strength with increasing numbers of plies in an LVL. However, the high variability observed during the tests does not allow definite conclusions to be drawn about this phenomenon.

On shear testing, some authors have found that shear modulus and shear strength decrease as the thickness of the veneers of the LVL increases (Norris et al. 1961; Ebihara 1981). However, Hoover et al. (1987) saw no significant effect of veneer thickness on shear strength. These contradictory results could be explained by a different quality of bonding and the greater or lesser importance of lathe checks from one case to another. In his thesis, El Haouzali (2009) shows an increase in shear strength according to the number of plies in the LVL with a MUF (Melamine Urea–Formaldehyde) glue, but a decrease with a PVAC (PolyVinyl ACetate) glue. The author notes that 'even though the interaction between these two effects (glue and thickness) is statistically significant, the differences noted remain very small'.

However, all the previous studies cited characterized LVLs with a constant laminate thickness while varying the ply thickness based on the number of plies. Only Lechner et al. (2021) have investigated specimens with a constant ply thickness, leading to LVLs with thickness increasing in correlation with the number of plies. Their tensile tests with 1-, 2-, and 4-ply specimens show an increase in failure stress and stiffness as the number of plies increases. Nevertheless, in the case of 6-ply LVL, the mechanical properties exhibit a lower average than the 4-ply version. The authors do not explain this decline in mechanical properties. Also, the study of the number of plies, at fixed

thickness, on the properties of LVLs, is barely treated in the literature so it is difficult to conclude at the moment.

In the case of carbon fibre reinforced composites (CFRP), the laminate theory model does not predict an increase in composite stiffness as the number of plies increases. Furthermore, studies by Nardone et al. (2012) and Gning et al. (2011) indicate no discernible impact of the number of plies on laminate stiffness. Nardone et al. (2012) studies laminates ranging from 1 to 3 plies, while Gning et al. (2011) studies laminates containing 2 to 10 plies.

It should be noted that few analytical models exist for LVL or plywood. However, since LVL and plywood are wood-based composites, i.e. a superposition of layers of wood veneers, many researchers use laminate theory to model these wood composites (Perry 1948; Okuma 1976; Cai and R. Dickens 2004; Yoshihara 2009, 2011; Wilczyński and Warmbier 2012; Makowski 2019). Some authors have developed analytical methods to model the mechanical properties and behaviour of LVL. Okuma (1976) proposes to model laminate by considering the effect of glue. To achieve this, he considers the part of the veneer where the glue penetrates the ply, leading to different mechanical properties. Wei et al. (2015, 2019) propose an improvement on this model, which, in addition to considering the addition of glue in the wood composite, also considers the densification of the plies related to the manufacturing of the LVL by pressing.

As shown by many authors (Okuma 1976; Wei et al. 2015; Gavrilović-Grmuša et al. 2016), LVL can be considered as a laminate composite of three materials:

- Veneers with an elastic modulus of E_w
- Glue with an elastic modulus of E_g
- A mixed wood-glue zone with an elastic modulus of E_m.

Note that, in the case of bonded wood joints, the mixed zone corresponds to an interface in which the wood cells are partially filled with adhesive (Marra 1992; Gavrilović-Grmuša et al. 2016). Penetration of the adhesive into the wood results in an increase in local stiffness and the formation of a wood-adhesive composite (Müller et al. 2009; Wei et al. 2015; Hunt et al. 2019). This mixed zone is often investigated in the case of glued wood joints when studying glue propagation (Marra 1992; Gavrilović-Grmuša et al. 2016). Based on a law of mixtures, Eq. (1) gives the value of the stiffness E_m (Wei et al. 2015).

$$E_m = E_w + rE_g \tag{1}$$

where

- E_m is the Young's modulus of the mixed wood-glue part in a given direction
- r is the proportion of void in the wood
- E_g is the Young's modulus of the glue in a given direction

E_w is the Young's modulus of wood in a given direction (Wei et al. 2015)

$$r = 1 - \frac{\rho_0}{\rho_f} \tag{2}$$

where

- ρ_0 is the density of oven-dried wood
- ρ_f is the cell wall density of dry wood

Five thicknesses are defined to describe the laminate studied. These thicknesses are shown in Fig. 1 and are noted as follows:

- t_g is the thickness of pure glue phase
- t_m is the thickness of the wood-glue mixture phase
- t_v is the thickness of the veneer in the LVL
- t_w is the thickness of the glue-free veneer
- t is the specimen thickness (not represented in Fig. 1)

It should be noted that the Young's modulus of the glue is highly dependent on the chemical formulation of the adhesive. In this study, single-component polyurethane-based (PUR 1C) adhesive was used to manufacture tensile specimens. However, the mechanical properties of polyurethane may vary depending of the chemical formulation of the resin (Müller et al. 2009). According to the literature, the Young's modulus of PUR glue ranges from 0.1 to 4 GPa (Konnerth et al. 2006; Clauβ et al. 2011; Stoeckel et al. 2013; Bockel et al. 2020).

Some authors also modelled LVLs based on the variations of fibre slopes measured on veneers, and also on the average density of the veneers. Each of these variables affects the mechanical properties of wood (Ross and Forest Products Laboratory USDA Forest Service 2010). Viguier et al. (2018) and Duriot (2021) proposed a model for the global Young's modulus by averaging the local stiffness of the veneers according to local fibre angles measured by the tracheid effect and the
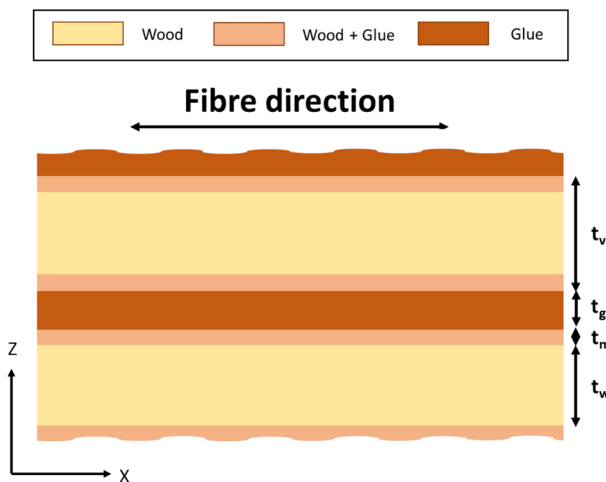

Fig. 1 Diagram showing the various materials of the laminate together and the different thicknesses notation used

mean density. The authors compared their model results with experimental values using four-point bending tests. They note that further studies are needed to validate this behaviour on LVLs and that taking the out-of-plane fibre angle into account and using local density mapping would provide more accurate results (Duriot 2021). Using the same principle, Ehrhart et al. (2021) took the slope of the fibre in the plane of the veneers into account to model their tensile strength.

The present study aims to continue the work carried out by the team since 2014 (Susainathan et al. 2020). LVLs made up of different poplar plies are being characterized through a series of uniaxial tensile tests. This campaign will help to understand and identify the mechanical properties of poplar LVL and its behaviour according to its number of plies.

Material and methods

Grain angle measurement

Koster poplar (*Populus x canadensis*) wood veneers, 1 mm thick, were used to manufacture the tensile test specimens. The veneers were produced and characterized by the LaBoMaP laboratory in Cluny using a wood lathe machine. The LaBoMaP provides a mapping of the in-plane fibre slope angle for each veneer, with a resolution of 2×2 mm^2. The in-plane slope of the fibre was obtained by the tracheid effect. When condensed light such as a laser beam is projected onto a wood surface, the beam is diffracted by the fibres and tracheids in the wood. This results in an elliptical light spot oriented in the same direction as the in-plane fibre slope (Daval et al. 2015). The fibre slope can then be calculated from the orientation of the ellipse formed by the observed light. Image analysis also made it possible to identify the light diffracted by fibres and thus the deviation of the wood grain to map these deviations in 2D. Figure 2 shows the location of the test specimen tabs (black in Fig. 2)
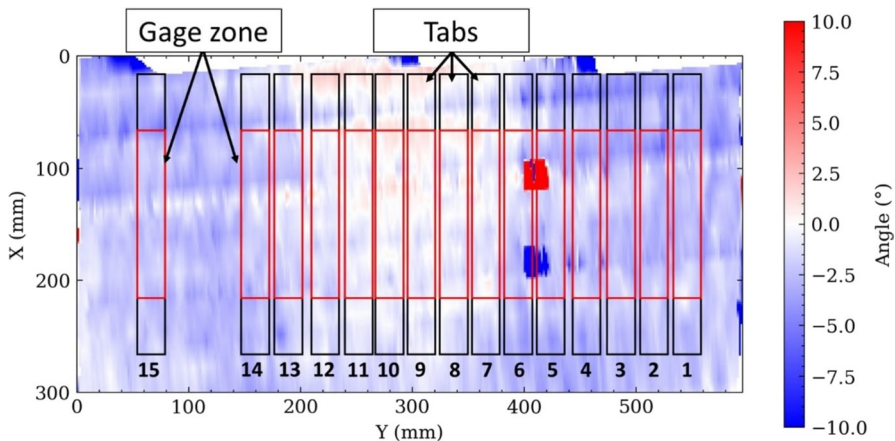

Fig. 2 Veneer mapping and specimen placement [0°]$_1$ (number beneath each specimen)

and the gage zone (red in Fig. 2) of each $[0°]_1$ test piece on the mapping of fibre angle of the veneer used to manufacture the test pieces.

Manufacturing of tensile specimens

The wood veneers were then glued using Kleiberit 510 PUR 1C FIBERBOND, stacked and pressed for 5 h at 10 bars and 25 °C to obtain the LVL. These LVLs were then cut into specimens to be characterized. The amount of glue used (recommended by the manufacturer) was 250 g/m². The density of poplar veneers was 355 kg/m³ with a Relative Standard Deviation (RSD) of 6%.

The manufacture process of veneers led to the formation of lathe checks on one of their sides called the Loose side (L), in contrast to the healthy side called the Tight side (T) (Perry 1948; Lutz 1974; Denaud et al. 2019). During stacking, faces with lathe checks are usually placed on healthy faces, except for outer plies, whose cracked faces face inward from the plywood. This stack is called 'tight side out and loose side in' and it is this assembly that is used in industry for the manufacture of plywood (Leggate et al. 2017).

Six 0° unidirectional specimen configurations were used for this study: $[0°]$, $[0°]_2$, $[0°]_3$, $[0°]_5$, $[0°]_7$, and $[0°]_9$. For $[0°]_2$ specimens, 3 different configurations were studied to characterize the influence of glued faces on tensile tests:

- Bonding on the tight sides ($[0°]_{2TT}$)
- Bonding of a tight side to a loose side ($[0°]_{2TL}$)
- Bonding on the loose sides ($[0°]_{2LL}$)

The influence of glued faces in LVL design has been studied by Blomqvist et al. (2014). However, these authors were only interested in the plane stability of the LVL. Li et al. (2020) looked at the influence of glued faces, but only on shear tests. The study of the influence of bonded faces on the in-plane stiffness of an LVL therefore remains to be characterized.

Three 90° unidirectional specimen configurations were also studied: $[90°]_3$, $[90°]_5$, and $[90°]_9$. These series were used to evaluate the effect of the number of plies on the transverse stiffness of LVL. A total of 15 specimens with rectangular geometry were made per configuration. The tensile specimens had nominal dimensions of 250×25×thickness of LVL mm³. Tabs, 50 mm long, were added at each end to limit stress concentrations and therefore breakage in the jaws of the testing machine. Two coordinate systems were employed to delineate the systems:

- A global reference frame (X,Y,Z) where X was aligned with the length of the specimen, Y corresponded to its width, and Z pertained to its thickness.
- A local reference frame (L,T,R), outlining the principal directions of the wood, to characterize the veneers (L aligned with the direction of the wood fibres or cells, R aligned with the growth rings, and T situated in the transverse direction within the plane of the veneers).

For $[0°]$ specimens, the two reference frames coincide. However, for $[90°]$ specimens, a 90° rotation around the Z (or R) axis is performed, aligning Y with L.

Experimental set-up

Tensile tests were performed at ambient temperature and humidity (23.6 °C and 64.6% RH). Wood samples were stabilized at 9.8% moisture content (Standard Deviation (SD): 0.28%). An Instron 5900 machine was used for these tests. A 50 kN force cell was installed, with a measurement accuracy of 0.5 N. The cross-head displacement rate applied was 2 mm/min. Stereo Digital Image Correlation (DIC) was used to track sample deformation. The use of DIC avoided the effect of any machine compliance that could have altered far-field strain measurements. Two 8 MP cameras (4096 × 2160 pixels) were used to acquire images of the specimens, which were painted with speckles for image correlation (Fig. 3). The black speckles were applied directly to the faces of the specimens, the bright sides of the poplar contrasting with the matte black paint. The speckles were made by spraying paint. The size of the patterns was determined according to the experimental set-up to obtain a minimum size of 3 pixels for each spot (Reu 2014) (Fig. 3).

A data acquisition system was used to record the load applied to the specimens with the same frequency as the DIC (2 Hz). Image correlation data were analysed with VIC-3D software. Calibration was carried out using a test pattern.
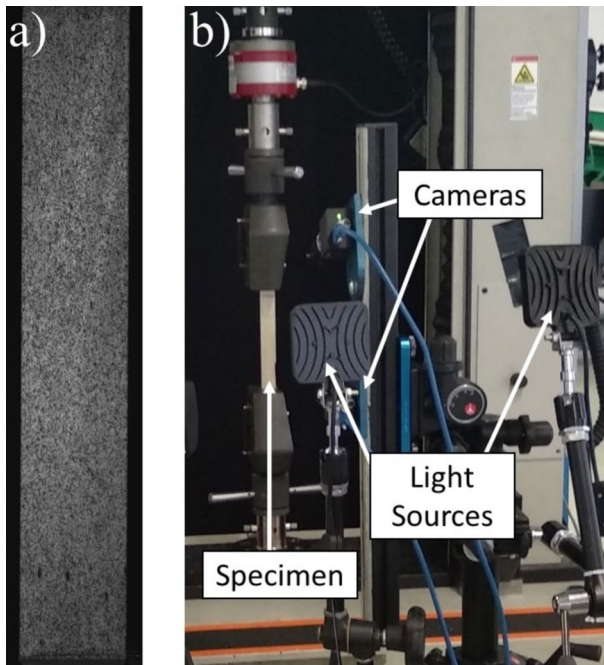

Fig. 3 Example of speckles on a specimen (**a**) and experimental set-up (**b**)

Methodology

Deformation calculation

For each specimen, mean strain was computed with DIC based on displacement of specific points as computed with a virtual extensometer. X and Y positions of 56 points were extracted from the image correlation data. Two lines of 20 points, spaced 16 mm apart, were used to calculate an average strain in the transverse direction Y (ε_{yy}) and two lines of 10 points, spaced 100 mm apart, were considered to calculate an average strain in the longitudinal direction X (ε_{xx}). The mean strain in the two plane directions of each specimen was based on the displacements of the points. The displacement measurement accuracy obtained is $8.0*10^{-5}$ mm along the X direction. The incertitude on ε_{xx} is therefore 1.6 μm/m. The displacement measurement accuracy obtained is $2.2*10^{-5}$ mm along the Y direction. The incertitude on ε_{yy} is therefore 2.8 μm/m.

Young's moduli and Poisson's ratio computation

Note that the longitudinal stiffness, the transverse stiffnesses, and the Poisson's ratio were calculated from the force measured in the tests, the averaged cross-sections (S) of the specimens measured at three points, and the mean strain computed by DIC based on standard ASTM D3039. By analysing data extracted from the longitudinal stress–strain curve between 1000 and 3000 μm/m, the ratio of stress changes to strain changes at these points was calculated. This ratio, found by dividing stress changes by strain changes, provided the Young's modulus for the respective direction. Similarly, Poisson's ratio was determined by dividing the negative transverse strain by the longitudinal strain within the same longitudinal strain range (1000 μm/m to 3000 μm/m).

Compression ratio (CR) computation

The wood density depends on many parameters such as its species, the presence of porosity, the presence of knots or various defects, the presence of resin or extractables, the ratio between final wood and initial wood or between sapwood and heartwood, and also temperature or humidity (Ross and Forest Products Laboratory USDA Forest Service 2010). Density is generally directly correlated with the mechanical properties of the wood: the denser the wood, the stiffer and stronger it is, regardless of the stress applied (Guitard 1987; Borrega and Gibson 2015; Trouy and Triboulot 2019). During the LVL manufacturing process, the use of presses to bond veneers can tend to densify the veneers. Densification occurs when the density of the veneer is artificially altered. It presents a pathway towards improving the mechanical characteristics of wood to a maximum density of about 1.5 g/cm^3, which corresponds to the cell wall density (Zobel and Jett 1995; Ross and Forest Products Laboratory USDA Forest Service 2010). Transverse or radial compression significantly reduces the volume of cell voids and is the most frequently used method for densifying wood (Jakob et al. 2022b). Although densification was not a specifically desired effect in

this work, when manufacturing LVLs, the pressure applied to glue the plies together tended to densify the LVL veneers. This densification affects the mechanical properties of LVL as the densification of the plies increases the stiffness and the failure stress of the LVL under bending, tensile and compression stresses (Lu et al. 2002; Bekhta et al. 2009; Kurt and Cil 2012; Gaff and Gašparík 2015; Pelit et al. 2018; Jakob et al. 2022a).

To characterize the mean compression of veneers in an LVL thickness (Z-direction) during the manufacturing, the compression ratio (CR) was identified. The compression ratio is calculated with Eq. 3 (Navi and Girardet 2000):

$$CR = \frac{\sum_{i=1}^{n} t_{ivi} - \sum_{i=1}^{n} t_{vi}}{\sum_{i=1}^{n} t_{ivi}} \tag{3}$$

where

- t_{ivi} is the initial thickness of veneer *i* before densification
- t_{vi} is the thickness of ply *i* in the LVL
- n is the number of plies in the LVL

In this study, control specimens were used to obtain a CR value for LVLs with 2, 3, 5, 7, and 9 plies. These control specimens had nominal dimensions of $400 \times 80 \times$ thickness of LVL mm^3. In this case, the manufacturing of the experimentally tested specimens was reproduced, and a precise 10-point measurement was made directly on the veneers used for the manufacture of LVL and then on the control specimens. The thickness of the pressed veneers was measured using a microscope directly on the LVL.

Knowing the thickness of the veneers before the LVL was made and the thickness of the veneers in the finished LVL, the value of CR corresponding to each veneer at 10 points was calculated with Eq. (3). The average CR value of the LVL was then the average of the CR values calculated for each veneer making up the wood composite. The geometry of the LVL plates used was different to facilitate measurement on all the pressed plates. In addition, the veneers used to make LVL were cut with a laser to remove any effect a mechanical cutting tool might have on the thickness at the edge of veneers. It was then assumed that the CR value obtained depended on the manufacturing process, and therefore that the CR values obtained from the control specimens were representative of the CR values of the LVL plates manufactured for the design of the tensile specimens.

A finite element model to assess the influence of fibre angle deviation

To exploit the measurement of in-plane fibre deviation in veneers and to study the influence of this deviation on the veneers' mechanical properties, a 2D finite element model was used to model the test specimens. The model was a linear 2D Finite Element Method (FEM) model of the gage zone of specimens considering the in-plane fibre angle for the calculation of the stiffness matrix of each element. The stiffness matrix for each element was computed according to laminate theory

(Berthelot 2005). The finite element model of each specimen consisted of ~ 13×75 elements, each element corresponding to a fibre angle measurement point on the veneer. For each specimen, a force was then applied to one edge of the specimen in the FEM model and the opposite edge was embedded across the entire width of the specimen. The input parameters of the finite element model were the longitudinal Young's modulus (E_l), the transverse Young's modulus (E_t), the plane shear elastic modulus (G_{lt}), the in-plane Poisson's ratio (ν_{lt}), and the fibre slope maps, previously obtained for each specimen by the tracheid effect. The output parameter studied in this article will be the stiffness of the specimen (E_x).

Modelling the tensile stiffness of LVLs

Even though Wei et al. (2015, 2019) have proposed an analytical model for plywood stiffness, they did not consider the glue joint when considering veneer compression. Yet, these two phenomena can take place simultaneously (Kurt and Cil 2012). To understand the effects of densification and glue during the manufacture of LVL, we propose some modifications to the analytical model developed by Wei et al. (2015). The model is based on a laminate theory and a mixture theory to account for the penetration of the glue into the wood (Wallace et al. 2019). During the veneer pressing process for LVL manufacture, the pressure exerted is directly linked to the thickness of the final glue joint. The stronger the pressure is, the thinner the glue joint will be and the more the glue will penetrate into the wood (Gavrilović-Grmuša et al. 2016). This is what Kurt and Cil (2012) show on LVLs assembled with PF glue. The thickness of the adhesive joint measured varies depending on the bonding conditions. The type of glue and its viscosity are parameters that affect the penetration of the glue into the wood (Hass 2012; Gavrilovic-Grmusa et al. 2012). Better impregnation of glue into wood leads to significant increases in hardness, compressive strength, flexural strength, and stiffness (Miroy et al. 1995; Nakata et al. 1997; Gindl and Gupta 2002; Furuno et al. 2004; Gindl et al. 2004; Shams et al. 2005; Kamke and Lee 2007; Kurt and Cil 2012). It should nevertheless be noted that, in the case of LVLs, a higher pressure during bonding will allow, not only better penetration of the glue, but also a densification of the plies (Kurt and Cil 2012). In the present model, it is assumed that the glue will propagate evenly into the wood plies to a depth of t_m. In practice, this is not the case, the distribution of the glue in the veneer is not homogeneous (Wang 2007). Starting from a theory of laminates, the longitudinal stiffness of LVL made of n plies can be defined as follows:

$$
\begin{aligned}
E &= E_g \sum_{i=1}^{n-1} \frac{t_g}{t} + 2E_m \sum_{i=1}^{n-1} \frac{t_m}{t} + E_w \sum_{i=1}^{n} \frac{t_w}{t} \\
&= \sum_{i=1}^{n-1} \left(\frac{t_g}{t} E_g + 2\frac{t_m}{t} E_m \right) + E_w \sum_{i=1}^{n} \frac{t_w}{t}
\end{aligned}
\tag{4}
$$

Using Eq. (1), we can write:

$$E = \sum_{i=1}^{n-1} \left(\frac{t_g}{t} E_g + 2 \frac{t_m}{t} \left[E_w + r E_g \right] \right) + E_w \sum_{i=1}^{n} \frac{t_w}{t}$$

$$= \frac{E_g}{t} \sum_{i=1}^{n-1} (t_g + 2 t_m r) + \frac{E_w}{t} \left[\sum_{i=1}^{n-1} 2 t_m + \sum_{i=1}^{n} t_w \right] \tag{5}$$

The sum of the veneer thicknesses is the sum of the thicknesses of the glue-free and glue-filled veneers. The following relationship can be established:

$$\sum_{i=1}^{n} t_v = \sum_{i=1}^{n-1} 2 t_m + \sum_{i=1}^{n} t_w \tag{6}$$

The relationship linking the glue spread of a bonded interface to the different thicknesses of the same interface, in the laminate, is defined as:

$$GS = [t_g + 2 t_m r] \rho_g \tag{7}$$

where

- GS is the glue spread, i.e. the mass of glue per m^2
- ρ_g is the density of the glue

Using Eqs. (5), (6), and (7) we can write:

$$E = \frac{E_g}{t} \sum_{i=1}^{n-1} \frac{GS}{\rho_g} + \frac{E_w}{t} \sum_{i=1}^{n} t_v$$

$$= \frac{(n-1) GS E_g}{t \rho_g} + \frac{n t_v E_w}{t} \tag{8}$$

In the case where the veneers are compressed during or before the manufacture of LVLs, the following relationship is established (Wei et al. 2015)

$$E_w = \frac{E_{w0}}{1 - CR} \tag{9}$$

where

- E_{w0} is the longitudinal Young's modulus of the wood before densification
- CR is the densification rate of the wood veneer

In contrast to Wei et al.'s approach (2015), the densification of veneers is taken into account while maintaining a non-zero glue joint in the analytical model here. In addition, the compression of the glue is not considered, as it can penetrate the voids of the wood freely during manufacture without being compressed. Using Eqs. (8) and Eq. (9), we can then write:

$$E = \frac{(n-1)GSE_g}{t\rho_g} + \frac{nt_vE_{w0}}{t(1-CR)}$$

$$= \frac{(n-1)GSE_g}{t\rho_g} + \frac{(t-(n-1)t_g)E_{w0}}{t(1-CR)} \qquad (10)$$

In Eq. (10), the first term corresponds to the influence of the glue on the stiffness of the laminate and the second to that of the wood plies. In this way, the formulation can be generalized for LVL or plywood of several species. It is then simple to adjust the formula to obtain the elastic tensile modulus of a given LVL or plywood:

$$E = \frac{(n-1)GSE_g}{t\rho_g} + \sum_{i=1}^{n} \frac{t_{vi}E_{0i}}{t(1-CR_i)} \qquad (11)$$

where

- t_{vi} is the thickness of ply i in the LVL
- E_{0i} is the longitudinal Young's modulus of ply i before densification
- CR_i is the compression ratio of ply i

In Eq. (11), the first term corresponds to the effect of the glue on the stiffness of the laminate, which depends on the amount of glue used to make the LVL and its physical and mechanical properties. The second term of the equation is a weighted average of the stiffness of the different compressed (or uncompressed) veneers. This term corresponds to the tensile strength of LVL based on laminate theory without considering the effect of glue in a wood composite.

Results

Study of specimens $[0°]_1$

Longitudinal Young's modulus of $[0°]_1$ specimens

The mean Young's modulus of $[0°]_1$ specimens was: $E_1 = 9299$ MPa (RSD: 17%). A strong variation was observed on the longitudinal Young's modulus $[0°]_1$ specimens. However, the variation observed was of the same order of magnitude as that observed by other authors on tensile tests on 1-ply 1 mm veneers (Pramreiter et al. 2021). In addition, the average stiffness value, obtained in these tests, was of the same order of magnitude as the values found in the literature. Studies have proposed a longitudinal Young's modulus value of 10,900 MPa for poplar when the wood has a moisture content of 12% (Ross and Forest Products Laboratory USDA Forest Service 2010) and 9260 MPa for a mature poplar with an average density of 0.433 g/cm^3 (Rahayu et al. 2015).

The observed variation can be explained by the density variation of the specimen characterized. The density of the wood in the $[0°]_1$ tensile specimens varied from

0.29 to 0.41 g/cm^3. A linear relationship with an r^2 coefficient of 0.82 is obtained between Young's modulus and density for the $[0°]_1$ specimens. It can be seen that the variation of the longitudinal Young's modulus in relation to the density (ρ) of the specimens is smaller than that of the Young's modulus alone: $E_1 = 9299$ MPa (RSD: 17%) and $E_1/\rho = 25{,}239$ MPa.cm^3/g (RSD: 8%).

During tensile testing of $[0°]_1$ specimens, the stiffness obtained is the specimen stiffness (E_x), not the fibre stiffness (E_1) because the fibre angle is not constantly equal to 0°. To determine fibre stiffness, specimen fibre slope mapping and FEM model were utilized. To characterize the influence of the fibre angle on the stiffness of the specimens, the parameters E_t, G_{lt}, and ν_{lt} were fixed: $E_t = 500$ MPa (average of the $[90°]_9$ series), $G_{lt} = 565$ MPa (values obtained from tests not presented in this article), and $\nu_{lt} = 0.48$ (average of the $[0°]_7$ and $[0°]_9$ series). Then the value of E_1 for each specimen was used as a variable so that the simulated stiffness of each specimen corresponded to the experimentally measured stiffness (E_x). The values of E_1 necessary for the simulated stiffness of each specimen to correspond to the stiffness measured experimentally, were always greater than the E_x. However, the distributions of E_x and E_1, and the variations were similar (17.65% for E_1 FEM versus 16.9% for E_x experimental). The variation was not significantly reduced when the fibre angle was considered in this case. Hence, the variation in fibre angle does not account for the disparities observed in specimen stiffness. In this study, specimens 5 and 6 were omitted because of fibre angle measurement problems (inconsistent measurement angles visible in Fig. 2).

Note that the in-plane fibre angles were quite low in this case, of the order of $\pm 3°$. Similar modelling has been carried out at the LaBoMaP in Cluny and their work shows that considering the measurement of the fibre slope makes it possible to explain a part of the variability in the elastic properties of veneers. However, the angles observed on their specimens were much greater due to the presence of knots ($\pm 30°$) (Viguier et al. 2018; Duriot 2021).

The variations observed on the longitudinal Young's modulus of the $[0°]_1$ specimens are mainly explained by the variability of the specimen density. The rest of the variation can be explained by the nature of the wood: wood veneer can be composed of earlywood (wood formed at the beginning of the growing season) and latewood (wood formed later in the season) (Stefanowski et al. 2020); the variability of the out-of-plane angle of the fibre; the variability of the local density of veneers or the presence of lathe checks.

Poisson's ratio of $[0°]_1$

The mean Poisson's ratio of the $[0°]_1$ specimens was $\nu_{lt} = 0.5$ (RSD: 27%). A strong variation in Poisson's ratio was observed on the $[0°]_1$ specimens. However, when the out-of-plane deformations of the specimens were observed during the tensile test, it could be seen that the specimens underwent cupping at the beginning of the test and tended to become flat before they failed (Figs. 4 and 5).

The cupping effect may be due to internal stresses in the veneer related to tension or compressive wood or variations in moisture or density in the wood (Blomqvist et al. 2014). The cupping effect was only observed on $[0°]_1$ specimens. Those
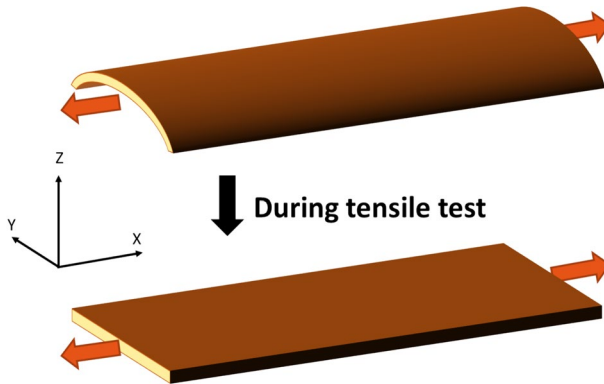
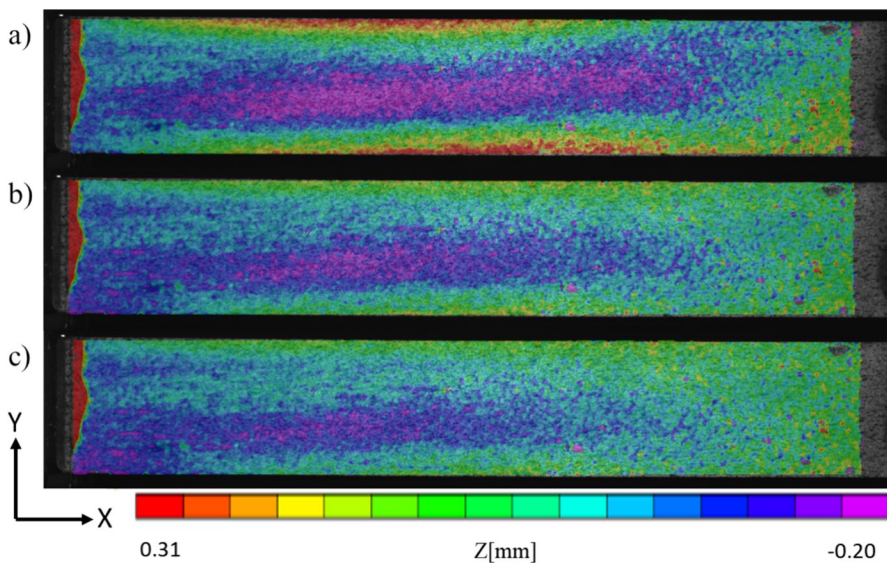**Fig. 4** Representation of the anti-cupping effect during tensile test

Fig. 5 Visualization of Z [mm] at the beginning (**a**), middle (**b**), and end of tests (**c**) on specimen No. 4 of the $[0°]_1$ series

specimens were thinner than those of the other series. Moreover, they were not glued and pressed. Such treatments could have added shape stability and limited the cupping effect.

During the tensile test, observing the out-of-plane position at every point of the specimen using the DIC analysis, allowed an anti-cupping behaviour to be visualized. It became evident that the cupping effect was more pronounced at the beginning of the tensile test ($\Delta z \sim 0.5$ mm) than towards the end of the test ($\Delta z \sim 0.2$ mm) (Fig. 5). It is supposed that this anti-cupping effect may explain the non-linearity of

the deformation along the Y-axis (Fig. 6). Because during the anti-cupping effect, one face of the specimen is affected by a transverse compression and the other undergoes a transverse tension during the tensile test. This phenomenon may therefore explain some of the variation in the values of the Poisson's ratio observed for these 1-ply specimens.

Considering that the cupping tends to cancel out at the end of the test, as observed on the out-of-plane displacement measurements (Fig. 5), an 'instantaneous' Poisson's ratio value can be computed by calculating the derivative: '$-d\varepsilon_{yy}/d\varepsilon_{xx}$' just before each specimen's failure. This results in a Poisson's ratio value of 0.66 (RSD: 15%). As ε_{xx} increases and tends to reach the failure of the specimen, the variation of the Poisson's ratio measured for the $[0°]_1$ series decreases. Then the value measurement tends toward the measurements of the Poisson's ratio on quasi-planar specimens, which explains this reduction in the observed variation. This cupping phenomenon is therefore a possible cause that would explain the variation of the Poisson's ratio measurements.

Study of $[0°]_2$ specimens

For $[0°]_2$ specimens, 3 different configurations were studied to characterize the influence of glued faces on tensile tests. At first glance, the analysis of the 2-ply specimens seems to show that the $[0°]_{2LL}$ specimens, i.e. specimens with the two lathe-checked faces glued to each other, are more rigid than the other series of 2-ply specimens (Fig. 7a).

The chart in Fig. 7 is a boxplot representation. This method of representing data makes it possible to compare the variation of several results on the same graphic. It can also be used to represent the median (green central lines in Fig. 7), quartiles 1 and 3 between which 50% of the measured values are included (black rectangles in Fig. 7), the min and max values of a sample (outer bounds in Fig. 7), and results that are abnormally far apart (points in Fig. 7) (Frigge et al. 1989).

Results were assessed statistically using the analysis of variance method–ANOVA (Fisher 1936)–at the 5% significance level. This statistical analysis is used to assess differences between three or more groups. If the probability that the differences are due to chance is less than 5% (significance threshold), it can be concluded that there is a significant difference between at least two groups. In this study, a significant difference was observed between the $[0°]_{2LL}$ series and the other two 2-ply series. It can therefore be concluded that the stiffness of the $[0°]_{2LL}$ series was significantly

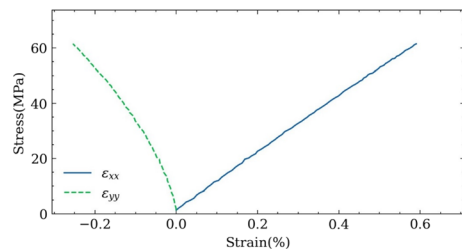**Fig. 6** Stress–strain curves for specimen No. 4 of the $[0°]_1$ series

Fig. 7 Distribution of the longitudinal Young's modulus by series (**a**), the Young's modulus multiplied ▶ by the cross-section and relative to the number of plies (**b**), and the specific Young's modulus multiplied by the cross-section and related to the number of plies (**c**)

higher than that of the other series. However, the thickness distribution shows that the $[0°]_{2LL}$ series is significantly thinner than the other two series (Fig. 8).

The hypothesis proposed is that the glue penetrated the wood thanks to lathe checks. The glue joint would therefore be thinner in this case (Fig. 9).

By measuring the control specimens, used for CR measurement, it was possible to measure the thickness of the veneers in the LVL at several points and to obtain an average value of the adhesive joints for each bonded interface. Figure 10 shows the distribution of adhesive joint thicknesses on the control specimens according to the faces glued. The proposed hypothesis therefore seems consistent. The glue joints seem to be thinner when the glued faces are cracked, the checks seem to contribute to the bonding. However, the high variability observed in the measurement of adhesive joints does not allow us to conclude on this influence.

In conclusion, the bonding method had a significant influence on the stiffness of the specimens at 5% only. However, this can be explained by the small thickness of the specimens $[0°]_{2LL}$. The difference in thickness may be related to the presence of lathe checks that facilitate the penetration of the adhesive into the veneers, thus reducing the thickness of the adhesive joint at the interface. However, there is no clear evidence to validate this hypothesis in this study.

Study of $[0°]_n$ specimens

The distribution of the mean Young's modulus of the $[0°]_n$ specimens is shown in Fig. 7. The variation observed on the longitudinal Young's modulus of the specimens $[0°]_n$ tends to decrease with the number of plies (Fig. 7a). In addition, there is a stiffening of the LVL depending on the number of plies. Young's modulus tends to increase with the number of plies when 2TT, 2LT, 3-, 5-, 7-, and 9-ply specimens are compared. The high variability of the $[0°]_1$ series does not allow it to be compared with the other series. This trend toward increasing stiffness is significant and is consistent with the results reported by Lechner et al. (2021) in tensile tests with 1-, 2-, and 4-ply specimens. It should be noted that the calculation of the stress used to calculate the stiffness of the veneers considers the cross-section measured on the tensile specimens.

Nevertheless, if the manufacturing process impacts the cross-section (such as veneer compression during LVL plate pressing), leading to alterations in specimen cross-sections, stress calculations may be affected by these changes. To overcome this problem, it is possible to compare the Young's modulus of the specimens by multiplying it by the cross-section of the specimens and dividing by the number of plies (for comparisons among the different series). Figure 7b illustrates this distribution according to the different series. A stiffening effect can still be seen when comparing the 2TT, 2LT, 3-, 5-, 7-, and 9-ply specimens.
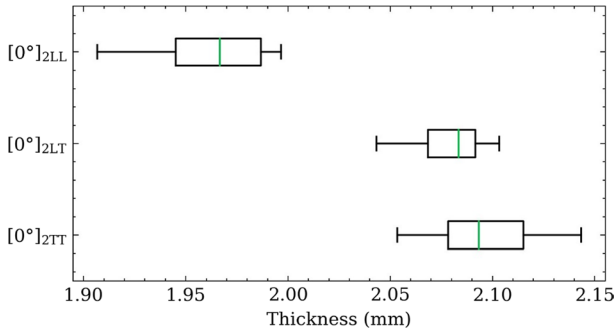
a)

b)

c)
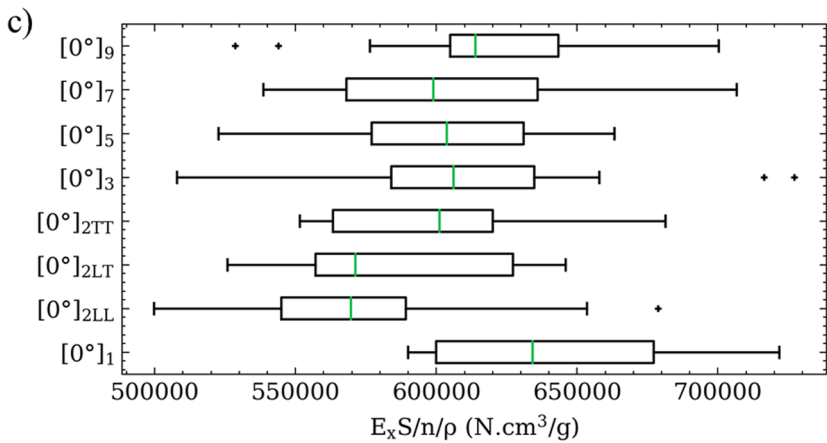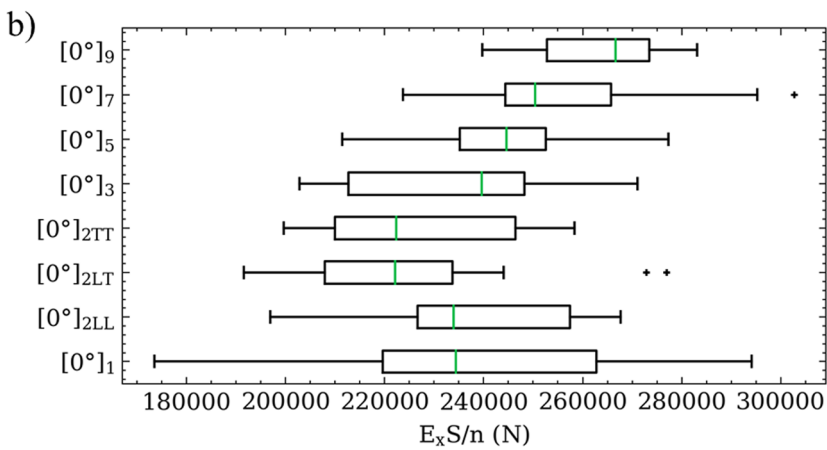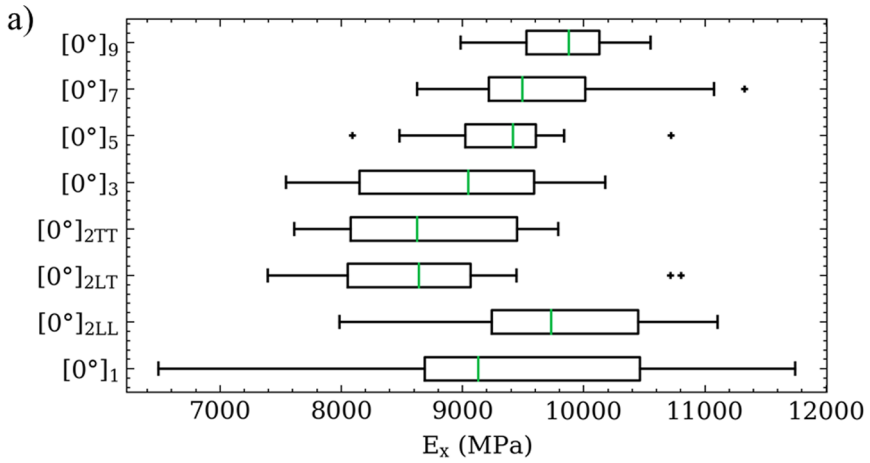
Fig. 8 Distribution of specimen thicknesses for 2-ply series
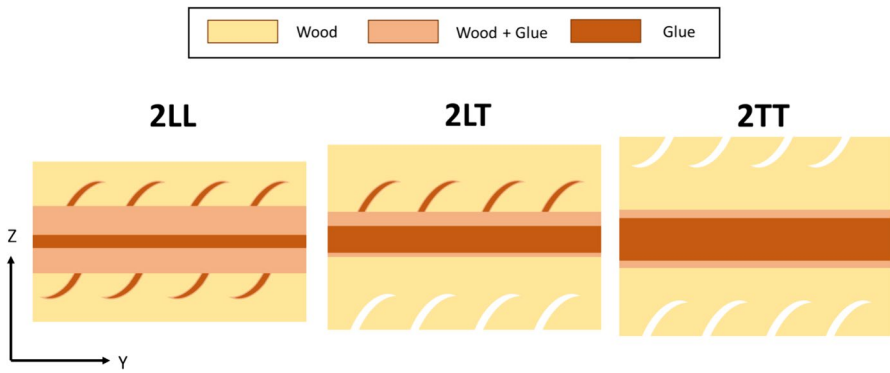

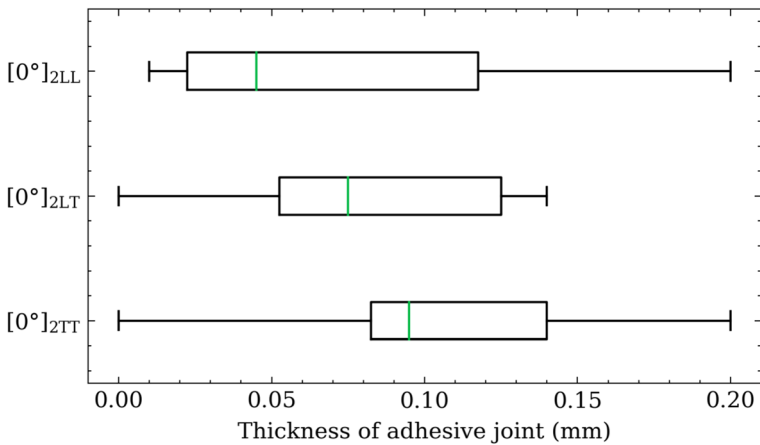**Fig. 9** Representation of glue propagation in specimens $[0°]_2$ according to faces glued

Fig. 10 Distribution of adhesive joint thicknesses for 2-ply series

To characterize the effect of density on the results obtained, the density of the wood of each specimen can be taken as the theoretical density of the wood composing the specimen. This density is calculated by subtracting the mass of glue used from the mass of the specimen manufactured and relating this mass to the volume of the specimen without considering the glue joints. It is assumed that the glue is homogeneously distributed over all the specimens of the same series.

It can be seen from Fig. 7c that the distribution of the specific longitudinal Young's modulus multiplied by the cross-section in relation to the number of plies in the specimens tends to be a constant function of the number of plies. The explanation for the observed increase in properties according to the number of plies can then be explained by the phenomenon of densification linked to the LVL manufacturing process. The role of glue in this increase in stiffness then seems of second-order.

However, as noted by some authors (Kiliç et al. 2006; Daoui et al. 2014), the thinner the LVL veneers, the greater the relative amount of glue used to manufacture the LVL. Table 1 summarizes the relative mass of the adhesive in each LVL plate used in the manufacture of the specimens. It can be seen that, from 5 plies on, the glue represents 1/3 of the mass of the LVL.

The ply number does not appear to affect the experimentally measured Poisson's ratio (ν_{lt}) values. However, increasing the number of plies tends to reduce the variability in the Poisson's ratio measurements but it has no influence on mean values obtained. This reduction in variation can be explained by the plane stability provided by the increase in the number of plies which tends to reduce the phenomenon of cupping in specimens (Blomqvist et al. 2014).

Study of $[90°]_n$ specimens

The distribution of the mean transverse Young's moduli of the $[90°]_n$ specimens is shown in Fig. 11. There is a stiffening of the LVL according to the number of plies. This stiffening is more significant than for $[0°]_n$ specimens.

Figure 12 shows that, in contrast to the $[0°]_n$ series, specific transverse Young's moduli multiplied by the cross-section relative to the number of plies of the specimens is always an increasing function of the number of plies. The increase observed in properties with the increasing number of plies can then be explained by the presence of glue in the LVL. In this configuration, the glue has a non-negligible effect on the stiffening of the specimens.

Since the transverse stiffness of poplar veneers is lower than the longitudinal stiffness, the stiffness of the glue added during the manufacture of LVLs plays a more important role in the total stiffness of the laminate.

Table 1 Relative percentage of glue in each LVL plate

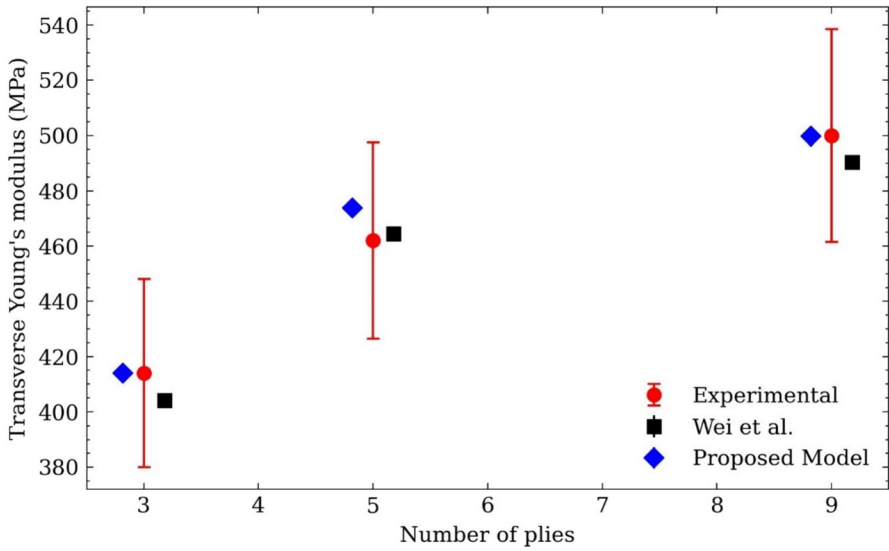| Number of plies	1	2	3	5	7	9
Relative mass of glue (%)	0	25%	31%	34%	36%	37%

Fig. 11 Comparison of Young's moduli for the $[90°]_n$ series between the analytical model and the experimental results (error bars represent standard deviation)

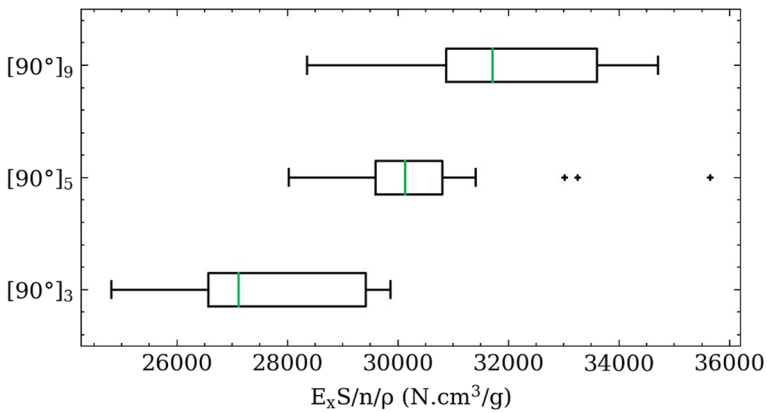**Fig. 12** Distribution of specific transverse Young's modulus times the cross-section and relative to the number of plies per series

CR values

To model the stiffness of experimentally characterized LVL, it is necessary to know the CR of veneers during LVL manufacturing. Table 2 summarizes the mean CR values obtained for each series based on measurements made on the control specimens.

Table 2 Summary of the different CR values according to the identification methods. The values in parentheses are the SDs

Number of plies	Reference CR (%) (and SD)
1	0
2LL	6.2 (2.8%)
2LT	8.6 (1.8%)
2TT	6.8 (3.5%)
3	9.1 (3.1%)
5	8.7 (4.8%)
7	8.2 (4%)
9	8.8 (4.1%)

Modelling

It was found that the average transverse and longitudinal stiffnesses increased with the number of plies (Figs. 7 and 11). To model these wood-based laminates, it was therefore necessary to take this stiffening into account when calculating the number of plies in an LVL. Based on the analytical model described above (Eq. 10), using the various measurements made on the specimens together with the CR values obtained from the control specimens, and estimating an E_g value, it is possible to compare the analytical model with the experimental values. The values of E_g and E_t are estimated using the $[90°]_3$ and $[90°]_9$ series to match the model and experimental values (Fig. 11). The $[90°]_3$ and $[90°]_9$ series were chosen because the former has the lowest relative mass of glue and the latter has the highest, so these series are the most relevant for identifying E_t and E_g respectively. The results are $E_g = 2170$ MPa and $E_t = 102$ MPa. This value of E_g is of the order of magnitude of the PUR adhesive stiffness values found in the literature (Stoeckel et al. 2013).

In the case of the $[90°]_n$ series, it can be seen that the proposed model is close to the one developed by Wei et al. (2019) (Fig. 11).

By using the value of E_g identified with the $[90°]_n$ series, it was then possible to model the $[0°]_n$ series. Note that the 2LL series was not part of the study because its stiffness is probably influenced by its small thickness, unlike the other 2-ply series, as explained above. The stiffness of the 2TT and 2LT series specimens was therefore averaged to obtain the stiffness of the series named $[0°]_2$.

It is considered that the stiffness of the $[0°]_1$ series follows a normal distribution with a mean of 9299 MPa and a standard deviation of 1556 MPa. Thus, since the choice of n veneers used to make LVL of a $[0°]_n$ series is independent and random, the stiffness of a $[0°]_n$ series also follows a normal distribution of mean 9299 MPa and standard deviation of $1556/\sqrt{n}$ MPa. This reduction in variability is well known in LVL manufacturing, one of the objectives of which is precisely the homogenization of mechanical properties. The LVL manufacturing process allows a better distribution of mechanical properties and natural defects, such as knots, grain slope or cracks in the wood composite (Leicester and Bunker 1969; Ebihara 1982; Youngquist et al. 1984; Sasaki and Abdullahi 2001; El Haouzali 2009; Erdil et al. 2009; Kiliç et al. 2010). This consideration of a theoretical

standard deviation allows us to account for a standard deviation in the analytical model to better compare this model to the experimental results (Fig. 13). The model proposed by Wei et al. (2015), considering the presence of a glue joint but not the compression of the veneers, is also shown in Fig. 13.

For the $[0°]_n$ series, the correlation between the proposed model and the experimental value is not as good as that found for the $[90°]_n$ series. This can be explained because the influence of the CR on this configuration is greater, even though its measurement is complex and a high variability is observed in the measurement (Table 2). However, the variability observed experimentally for each series agrees with the one obtained with the analytical model.

On average, Wei's theory shows smaller deviations from the experimental values. However, it should be noted that there is a high variability in compression ratio measurements which have a significant effect on the analytical results in this study. Better control and measurement of CR could help to refine the results obtained. Nevertheless, the model offered more possibilities by allowing both the densification of veneers and the presence of glue joints in wood composites to be modelled. In addition, the model accounts for the variability observed experimentally. Finally, it should be noted that the differences observed between the analytical modelling and the experimental tests are close to or even smaller than the variability observed experimentally which allows us to validate this model. It is also important to note that the model used is very close to the experimental results for 7- and 9-ply specimens (error of less than 3% on average), whereas industrial LVL are mostly composed of 8 or more plies (Finnish Woodworking Industries Federation 2019).
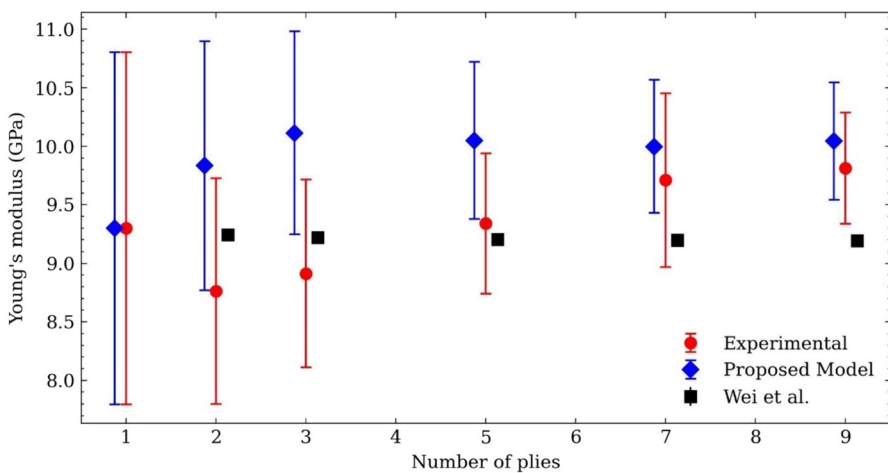

Fig. 13 Comparison of Young's moduli for the $[0°]_n$ series between the analytical model and experimental results (error bars represent standard deviation)

Discussion

Tensile tests on 1-, 2-, 3-, 5-, 7-, and 9-ply poplar LVLs were carried out to characterize the transverse and longitudinal stiffness of these laminates and the influence of the number of plies. The results show that stiffness tends to increase when the laminate is composed of a sufficient number of plies. This observation is valid, not only for longitudinal stiffness but also for transverse stiffness where the effect is even greater. A variant of Wei et al.'s (2015) model is proposed to account for this behaviour. Although Lechner et al. (2021) had already been able to observe this phenomenon, they did not explain it. The explanations on the increase in stiffness put forward during this work are based on the LVL manufacturing process: when the number of plies is increased, the relative amount of glue in the laminate increases.

However, given the results presented, it should be borne in mind that the method used to measure the compression ratio of veneers is open to discussion. Measuring the compression ratio (CR) during manufacturing by assessing the thicknesses of plate edges before pressing/gluing the LVL does not provide precise CR values for individual plies in each specimen. However, employing control LVLs allows more accurate measurements of veneers to be made both before and after pressing/gluing, all at a single location, offering a distinct advantage. However, the value obtained from the compression ratio may not be exactly that of the plates manufactured for specimen design (e.g. due to scale effect) and densification may be variable under the press.

The stiffness of the adhesive (E_g), which has been indirectly identified with the $[90°]_n$ series, can also affect the analysis performed. However, the phenomenon of interaction between glue and wood is still considered complex, so it remains an area of active research even today. Nevertheless, it can be noted that the stiffness identified via the proposed analytical model and the $[90°]_n$ tests allows us to identify a stiffness value of the order of 1.8 GPa for the adhesive. This value is well within the range of values obtained in the literature. In addition, this stiffness of 1.8 GPa helps to explain why the glue has a greater effect on the stiffening of $[90°]_n$ specimens than on that of $[0°]_n$ specimens. In the case of $[90°]_n$ specimens, the glue is almost 12 times as stiff as the 90° plies while, for the $[0°]_n$ series, the 0° plies are only 5 times as stiff as the glue.

Conclusion and perspectives

The effects of the number of plies on the stiffness of an LVL were studied in tensile tests on LVLs of 1, 2, 3, 5, 7, and 9 plies. The following conclusions can be drawn from the results of the study:

- A high variation (17%) is observed on the stiffness of the $[0°]_1$ specimens, but the density of the specimens explains half of this variation.

- The influence of the low in-plane fibre slope on the variation of the stiffness measured for the $[0°]_1$ specimens is very slight.
- High variation (27%) is observed on the measurement of the Poisson's ratio of $[0°]_1$ specimens, based on the measurement proposed by ASTM D3039. The out-of-plane deformation and anti-cupping effect of the specimens during the tensile test seems to explain this high measurement variation. A variation of 16% is obtained by using the end of the tensile test to calculate the Poisson's ratio.
- For the $[0°]_2$ specimens, the stiffness of the $[0°]_{2LL}$ series is higher than that of the other series. However, no significant difference in specific stiffness was observed between the series of two plies, depending on the faces that were glued.
- An increase in stiffness is observed as the number of plies composing the LVL increases for the $[0°]_n$ and $[90°]_n$ specimens. A model has been proposed to account for this phenomenon. This analytical model considers the compression of the veneers and the presence of glue joints in the LVL. It gives the best result for the $[90°]_n$ configuration, since it is in this direction of stress that the increase in stiffness with the number of plies is greatest.
- The model presented in this article builds upon existing papers focusing on modelling LVL stiffness. It offers a generalized approach compared to previous efforts, enabling the incorporation of factors such as glue, compression ratio, and plies with diverse orientations, thicknesses, and properties. Additionally, the final formulation relies on easily identifiable parameters.
- In the specimens characterized, the more plies there were in an LVL, the more the variation of the elastic modulus seemed to decrease. The stiffness observed on tensile tests was more homogeneous.

The study of the stiffness of an LVL according to the number of plies composing it provides a better understanding of the link between manufacturing and the mechanical properties of the material. To set up a digital wood-based composite model, this information seems relevant. However, more research is needed to determine the influence of the number of plies for different orientations, materials and adhesives. Consideration of local density or lathe checks could help to explain some of the variability observed in these tests. In addition, studies on various resources could validate the behaviour observed on species other than poplar.

Author contribution Axel Peignon is the first author, responsible for sample preparation and testing, data analysis, and the preparation of the paper. Joël Serra provided technical support in tensile testing, data analysis, and comments for the paper. Florent Eyma and Arthur Cantarel provided technical guidance for the research and the preparation of the paper. Bruno Castanié is the corresponding author and provided technical guidance for the research and the preparation of the paper.

Data availability No datasets were generated or analysed during the current study.

Declarations

Conflict of interest The authors declare that they have no known competing financial interests or personal relationships that could appear to influence the work reported in this paper.

References

Acosta R, Montoya JA, Welling J (2021) Determination of the suitable shape for tensile tests parallel to the fibers in Guadua angustifolia Kunth specimens. BioResources 16:3214–3223. https://doi.org/10.15376/biores.16.2.3214-3223

AURA AERO. (2023) In: Aura Aero. https://aura-aero.com/. Accessed 16 May 2023

Balduzzi G, Zelaya-Lainez L, Hochreiner G, Hellmich C (2021) Dog-bone samples may not provide direct access to the longitudinal tensile strength of clear-wood. Open Civ Eng J 15:1–12. https://doi.org/10.2174/1874149502115010001

Bekhta P, Hiziroglu S, Shepelyuk O (2009) Properties of plywood manufactured from compressed veneer as building material. Mater Des 30:947–953. https://doi.org/10.1016/j.matdes.2008.07.001

Berthelot J-M (2005) Matériaux composites: comportement mécanique et analyse des structures, Composite materials: Mechanical behavior and structural analysis , 4e édition. Tec & Doc Lavoisier

Blomqvist L, Sandberg D, Johansson J (2014) Influence of veneer orientation on shape stability of plane laminated veneer products. Wood Mater Sci Eng 9:224–232. https://doi.org/10.1080/17480272.2014.919022

Bockel S, Harling S, Grönquist P, et al. (2020) Characterization of wood-adhesive bonds in wet conditions by means of nanoindentation and tensile shear strength. Eur J Wood Prod 12

Borrega M, Gibson LJ (2015) Mechanics of balsa (*Ochroma pyramidale*) wood. Mech Mater 84:75–90

Cai Z, Dickens JR (2004) Wood composite warping: modeling and simulation. Wood Fiber Sci 36:174–185

Castanié B, Bouvet C, Ginot M (2020) Review of composite sandwich structure in aeronautic applications. Compos Part C Open Access 1:100004. https://doi.org/10.1016/j.jcomc.2020.100004

Castanié B et al (2024) Wood and plywood as eco-materials for sustainable mobility: A review. Compos Struct 329:117790

Clauβ S, Dijkstra DJ, Gabriel J et al (2011) Influence of the chemical structure of PUR prepolymers on thermal stability. Int J Adhes Adhes 31:513–523. https://doi.org/10.1016/j.ijadhadh.2011.05.005

Daoui A, Descamps C, Marchal R, Zerizer A (2011) Influence of veneer quality on beech LVL mechanical properties. Maderas Cienc Tecnol 13:69–83. https://doi.org/10.4067/S0718-221X2011000100007

Daoui A, Descamps C, Zerizer A et al (2014) Variation de l'épaisseur du placage de déroulage des bois et son influence sur les caractéristiques mécaniques des panneaux LVL, Variation in peeling veneer thickness and its influence on the mechanical properties of LVL panels. MATEC Web Conf 11:01041. https://doi.org/10.1051/matecconf/20141101041

Darmawan W, Nandika D, Massijaya Y et al (2015) Lathe check characteristics of fast growing sengon veneers and their effect on LVL glue-bond and bending strength. J Mater Process Technol 215:181–188. https://doi.org/10.1016/j.jmatprotec.2014.08.015

Daval V, Pot G, Belkacemi M et al (2015) Automatic measurement of wood fiber orientation and knot detection using an optical system based on heating conduction. Opt Express 23:33529. https://doi.org/10.1364/OE.23.033529

Denaud L, Marcon B, Rohumaa A, et al. (2019) Influence of peeling process parameters on veneer lathe check properties. Corvallis, OR, USA

Duriot R (2021) Développement de produits LVL de douglas aux propriétés mécaniques optimisées par l'exploitation de la mesure en ligne de l'orientation des fibres lors du déroulage, Development of LVL Douglas Fir products with optimized mechanical properties using on-line measurement of fiber orientation during peeling . PhD Thesis

Ebihara T (1981) Shear properties of laminated-veneer lumber (LVL). J Jpn Wood Res Soc Jpn

Ebihara T (1982) The performance of composite beams with laminated-veneer lumber (LVL) flanges. J Jpn Wood Res Soc Jpn

Ehrhart T, Palma P, Schubert M et al (2021) Predicting the strength of European beech (*Fagus sylvatica* L.) boards using image-based local fibre direction data. Wood Sci Technol 56:123–146. https://doi.org/10.1007/s00226-021-01347-w

Erdil Y, Kasal A, Zhang J et al (2009) Comparison of mechanical properties of solid wood and laminated veneer lumber fabricated from turkish beech, scotch pine, and lombardy poplar. For Prod J 59:55–60

Federation FWI (ed) (2019) LVL handbook Europe. Federation of the Finnish woodworking industries, Helsinki

Fisher RA (1936) Statistical methods for research workers. Stat Methods Res Work

Frigge M, Hoaglin DC, Iglewicz B (1989) Some Implementations of the Boxplot. Am Stat 43:50–54. https://doi.org/10.1080/00031305.1989.10475612

Furuno T, Imamura Y, Kajita H (2004) The modification of wood by treatment with low molecular weight phenol-formaldehyde resin: a properties enhancement with neutralized phenolic-resin and resin penetration into wood cell walls. Wood Sci Technol 37:349–361. https://doi.org/10.1007/s00226-003-0176-6

Gaff M, Gašparík M (2015) Influence of densification on bending strength of laminated beech wood. BioResources 10:1506–1518. https://doi.org/10.15376/biores.10.1.1506-1518

Gavrilovic-Grmusa I, Dunky M, Miljkovic J, Djiporovic-Momcilovic M (2012) Influence of the viscosity of UF resins on the radial and tangential penetration into poplar wood and on the shear strength of adhesive joints. Holzforschung 66:849–856. https://doi.org/10.1515/hf-2011-0177

Gavrilović-Grmuša I, Dunky M, Djiporović-Momčilović M et al (2016) Influence of pressure on the radial and tangential penetration of adhesive resin into poplar wood and on the shear strength of adhesive joints. BioResources 11:2238–2255. https://doi.org/10.1537/biores.11.1.2238-2255

Gindl W, Gupta HS (2002) Cell-wall hardness and Young's modulus of melamine-modified spruce wood by nano-indentation. Compos Part Appl Sci Manuf 33:1141–1145. https://doi.org/10.1016/S1359-835X(02)00080-5

Gindl W, Gupta HS, Schöberl T et al (2004) Mechanical properties of spruce wood cell walls by nanoindentation. Appl Phys A 79:2069–2073. https://doi.org/10.1007/s00339-004-2864-y

Gindl W, Sretenovic A, Vincenti A, Müller U (2005) Direct measurement of strain distribution along a wood bond line. Part 2: effects of adhesive penetration on strain distribution. Holzforschung 59:307–310. https://doi.org/10.1515/HF.2005.051

Gning PB, Liang S, Guillaumat L, Pui WJ (2011) Influence of process and test parameters on the mechanical properties of flax/epoxy composites using response surface methodology. J Mater Sci 46:6801–6811. https://doi.org/10.1007/s10853-011-5639-9

Guélou R, Eyma F, Cantarel A et al (2021a) Static crushing of wood based sandwich composite tubes. Compos Struct. https://doi.org/10.1016/j.compstruct.2021.114317

Guélou R, Eyma F, Cantarel A et al (2021b) Crashworthiness of poplar wood veneer tubes. Int J Impact Eng 147:103738. https://doi.org/10.1016/j.ijimpeng.2020.103738

Guélou R, Eyma F, Cantarel A et al (2022a) A comparison of three wood species (poplar, birch and oak) for crash application. Eur J Wood Prod. https://doi.org/10.1007/s00107-022-01871-x

Guélou R, Eyma F, Cantarel A et al (2022b) Dynamic crushing of wood-based sandwich composite tubes. Mech Adv Mater Struct 29:7004–7024. https://doi.org/10.1080/15376494.2021.1991533

Guitard D (1987) Mécanique du matériau bois et composites, Mechanics of wood and composite materials. Daniel Guitard

H'ng PS, Paridah MT, Chin KL (2010) Bending properties of laminated veneer lumber produced from Keruing (Dipterocarpus sp.) Reinforced with Low Density Wood Species. Asian J Sci Res. https://doi.org/10.3923/ajsr.2010.118.125

El Haouzali H (2009) Déroulage du peuplier : effets cultivars et stations sur la qualité des produits dérivés, Poplar pulping: cultivar and site effects on by-product quality. Phd Arts et Métiers Paris-Tech. https://pastel.hal.science/pastel-00005567215

Hass PFS (2012) Penetration behavior of adhesives into solid wood and micromechanics of the bondline. PhD Thesis, ETH Zurich

Hoover WL, Ringe JM, Eckelman CA, Youngquist JA (1987) Material design factors for hardwood laminated-veneer-lumber. For Prod J 37:5

Hunt CG, Frihart CR, Dunky M, Rohumaa A (2019) Understanding wood bonds-going beyond what meets the eye: a Critical review. In: Mittal KL (ed) Progress in adhesion and adhesives, 1st edn. Wiley, pp 353–419

Jakob M, Czabany I, Veigel S et al (2022a) Comparing the suitability of domestic spruce, beech, and poplar wood for high-strength densified wood. Eur J Wood Prod 80:859–876. https://doi.org/10.1007/s00107-022-01828-0

Jakob M, Mahendran AR, Gindl-Altmutter W et al (2022b) The strength and stiffness of oriented wood and cellulose-fibre materials: a review. Prog Mater Sci 125:100916. https://doi.org/10.1016/j.pmatsci.2021.100916

Jeong GY, Zink-Sharp A, Hindman DP (2010) Applying digital image correlation to wood strands: influence of loading rate and specimen thickness. Holzforschung 64:729–734. https://doi.org/10.1515/hf.2010.110

Kamke FA, Lee JN (2007) Adhesive penetration in wood–a review. Wood Fiber Sci, 205–220

Kiliç Y, Colak M, Baysal E, Burdurlu E (2006) An investigation of some physical and mechanical properties of laminated veneer lumber manufactured from black alder (AInus glutinosa) glued with polyvinyl acetate and polyurethane adhesives. For Prod Soc 56:5

Kiliç Y, Burdurlu E, Elibol G, Ulupinar M (2010) Effect of layer arrangement on expansion, bending strength and modulus of elasticity of solid wood and laminated veneer lumber (LVL) produced from pine and poplar. Gazi Univ J Sci 23:89–96

Kläusler O, Clauß S, Lübke L et al (2013) Influence of moisture on stress–strain behaviour of adhesives used for structural bonding of wood. Int J Adhes Adhes 44:57–65. https://doi.org/10.1016/j.ijadhadh.2013.01.015

Konnerth J, Jäger A, Eberhardsteiner J et al (2006) Elastic properties of adhesive polymers. II. Polymer films and bond lines by means of nanoindentation. J Appl Polym Sci 102:1234–1239. https://doi.org/10.1002/app.24427

Konnerth J, Gindl W, Müller U (2007) Elastic properties of adhesive polymers. I. Polymer films by means of electronic speckle pattern interferometry. J Appl Polym Sci 103:3936–3939. https://doi.org/10.1002/app.24434

Kurt R, Cil M (2012) Effects of press pressures on glue line thickness and properties of laminated veneer lumber glued with phenol formaldehyde adhesive. BioResources 7:5346–5354. https://doi.org/10.15376/biores.7.4.5346-5354

Lechner M, Dietsch P, Winter S (2021) Veneer-reinforced timber–numerical and experimental studies on a novel hybrid timber product. Constr Build Mater 298:123880. https://doi.org/10.1016/j.conbuildmat.2021.123880

Leggate W, McGavin R, Bailleres H (2017) A guide to manufacturing rotary veneer and products from small logs, ACIAR Monograph. https://www.aciar.gov.au/publication/books-and-manuals/guide-manufacturing-rotary-veneer-and-products-small-logs

Leicester RH, Bunker RC (1969) Fracture at butt joints in laminated pine. For Prod J 19:59–60

Li W, Zhang Z, He S et al (2020) The effect of lathe checks on the mechanical performance of LVL. Eur J Wood Prod 78:545–554. https://doi.org/10.1007/s00107-020-01526-9

Lu X, Chen Y, Chen Y (2002) The prediction of elastic modulus along the grain of poplar veneer. J Nanjing for Univ 45:9. https://doi.org/10.3969/j.jssn.1000-2006.2002.03.004

Lutz JF (1974) Techniques for peeling, slicing and drying veneer. Forest Products Laboratory, Forest Service, USDA, USA

Mair-Bauernfeind C, Zimek M, Asada R et al (2020) Prospective sustainability assessment: the case of wood in automotive applications. Int J Life Cycle Assess 25:2027–2049. https://doi.org/10.1007/s11367-020-01803-y

Makowski A (2019) Analytical analysis of distribution of bending stresses in layers of plywood with numerical verification. Drv Ind 70:77–88. https://doi.org/10.5552/drvind.2019.1823

Marra AA (1992) Technology of wood bonding: principles in practice. Van Nostrand Reinhold, New York

Miroy F, Eymard P, Pizzi A (1995) Wood hardening by methoxymethyl melamine. Holz Roh- Werkst 53:276–276. https://doi.org/10.1007/s001070050089

Müller U, Veigel S, Follrich J, et al. (2009) Performance of one component polyurethane in comparison to other wood adhesives. Lake Tahoe, Nevada, USA

Nakata K, Sugimoto H, Inoue M, Kawai S (1997) Development of compressed wood fasteners for timber construction. I. Mechanical properties of phenolic resin impregnated compressed laminated veneer lumber. Dev Compress Wood Fasten Timber Constr Mech Prop Phenolic Resin Impregn Compress Laminated Veneer Lumber 43:38–45

Nardone F, Di Ludovico M, De Caso Y, Basalo FJ et al (2012) Tensile behavior of epoxy based FRP composites under extreme service conditions. Compos Part B Eng 43:1468–1474. https://doi.org/10.1016/j.compositesb.2011.08.042

Navi P, Girardet F (2000) Effects of thermo-hydro-mechanical treatment on the structure and properties of wood. Holzforschung 54:287–293. https://doi.org/10.1515/HF.2000.048

Norris CB, Werren F, McKinnon PF (1961) The effect of veneer thickness and grain direction on the shear strength of plywood. [Govt. print. off, Washington

Okuma M (1976) Plywood properties influenced by the glue line. Wood Sci Technol 10:57–68. https://doi.org/10.1007/BF00376385

Peignon A, Serra J, Gélard L et al (2023) Mode I delamination R-Curve in poplar laminated veneer lumber. Theor Appl Fract Mech. https://doi.org/10.1016/j.tafmec.2023.103982

Pelit H, Budakçı M, Sönmez A (2018) Density and some mechanical properties of densified and heat post-treated Uludağ fir, linden and black poplar woods. Eur J Wood Prod 76:79–87. https://doi.org/10.1007/s00107-017-1182-y

Perry TD (1948) Modern plywood

Pramreiter M, Stadlmann A, Huber C et al (2021) The influence of thickness on the tensile strength of finnish birch veneers under varying load angles. Forests 12:87. https://doi.org/10.3390/f12010087

Rahayu I, Denaud L, Marchal R, Darmawan W (2015) Ten new poplar cultivars provide laminated veneer lumber for structural application. Ann Sci 72:705–715. https://doi.org/10.1007/s13595-014-0422-0

Reu P (2014) All about speckles: speckle Size Measurement. Exp Tech 38:1–2. https://doi.org/10.1111/ext.12110

Ross RJ, Forest Products Laboratory USDA Forest Service (2010) Wood handbook: wood as an engineering material. Forest products laboratory, Madison, WI

Sasaki H, Abdullahi AA (2001) Lumber: laminated veneer. In: Buschow KHJ (ed) Encyclopedia of materials: science and technology. Elsevier, Amsterdam, pp 4678–4680

Schaffer EL, Jokerst RW, Moody RC, et al. (1972) Feasibility of Producing a High-Yield Laminated Structural Product. 23

Shams MdI, Yano H, Endou K (2005) Compressive deformation of wood impregnated with low molecular weight phenol formaldehyde (PF) resin III: effects of sodium chlorite treatment. J Wood Sci 51:234–238. https://doi.org/10.1007/s10086-004-0638-y

Shupe TF, Hse C-Y, Choong ET, Groom LH (1998) Effects of silvicultural practice and moisture content level on lobolly pine veneer mechanical properties. For Prod J 47(11/12):92–96

Stefanowski S, Frayssinhes R, Pinkowski G, Denaud L (2020) Study on the in-process measurements of the surface roughness of Douglas fir green veneers with the use of laser profilometer. Eur J Wood Prod 78:555–564. https://doi.org/10.1007/s00107-020-01529-6

Stoeckel F, Konnerth J, Gindl-Altmutter W (2013) Mechanical properties of adhesives for bonding wood–a review. Int J Adhes Adhes 45:32–41. https://doi.org/10.1016/j.ijadhadh.2013.03.013

Susainathan J, Eyma F, De Luycker E et al (2019) Experimental investigation of compression and compression after impact of wood-based sandwich structures. Compos Struct 220:236–249. https://doi.org/10.1016/j.compstruct.2019.03.095

Susainathan J, Eyma F, De Luycker E et al (2020) Numerical modeling of impact on wood-based sandwich structures. Mech Adv Mater Struct 27:1583–1598. https://doi.org/10.1080/15376494.2018.1519619

Trouy M-C, Triboulot P (2019) Matériau bois–structure et caractéristiques, " Wood material–structure and characteristics ". Superstructures Bâtim. https://doi.org/10.51257/a-v4-c925

Viguier J, Bourgeay C, Rohumaa A et al (2018) An innovative method based on grain angle measurement to sort veneer and predict mechanical properties of beech laminated veneer lumber. Constr Build Mater 181:146–155. https://doi.org/10.1016/j.conbuildmat.2018.06.050

Wallace CA, Saha GC, Afzal MT, Lloyd A (2019) Experimental and computational modeling of effective flexural/tensile properties of microwave pyrolysis biochar reinforced GFRP biocomposites. Compos Part B Eng 175:107180. https://doi.org/10.1016/j.compositesb.2019.107180

Wang BJ (2007) Experimentation and modeling of hot pressing behaviour of veneer-based composites. PhD Thesis, University of British Columbia

Wei P, Rao X, Wang BJ, Dai C (2015) A modified theory of composite mechanics to predict tensile modulus of resinated wood. Wood Res 60:16

Wei P, Wang BJ, Wan X, Chen X (2019) Modeling and prediction of modulus of elasticity of laminated veneer lumber based on laminated plate theory. Constr Build Mater 196:437–442. https://doi.org/10.1016/j.conbuildmat.2018.11.137

Wilczyński M, Warmbier K (2012) Elastic moduli of veneers in pine and beech plywood. Drew Pr Nauk Doniesienia Komun 55:47–57

Wood CAR (2021) https://www.woodcar.eu/. Accessed 22 Nov 2021

Wu Q, Cai Z, Lee JN (2005) Tensile and dimensional properties of wood strands made from plantation southern pine lumber. For Prod J 55(2):87–92

Yoshihara H (2009) Poisson's ratio of plywood measured by tension test. Holzforschung 63(5):603–608. https://doi.org/10.1515/HF.2009.092

Yoshihara H (2011) Measurement of the in-plane shear modulus of plywood by tension test of [±45] off-axis specimen. Trans Jpn Soc Mech Eng Ser A 77:670–678. https://doi.org/10.1299/kikaia.77.670

Youngquist JA, Laufenberg TL, Bryant BS (1984) End jointing of laminated veneer lumber for structural use. For Prod J 34:25–32

Zobel BJ, Jett JB (1995) The importance of wood density (specific gravity) and its component parts. Genetics of wood production. Springer, Berlin Heidelberg, pp 78–97